Yadav, Karan; Kumar, Bhavnesh; Devaraju, Swaroop

Article

Mitigation of Mismatch Power Losses of PV Array under Partial Shading Condition using novel Odd Even Configuration

Energy Reports

Provided in Cooperation with:
Elsevier

Suggested Citation: Yadav, Karan; Kumar, Bhavnesh; Devaraju, Swaroop (2020) : Mitigation of Mismatch Power Losses of PV Array under Partial Shading Condition using novel Odd Even Configuration, Energy Reports, ISSN 2352-4847, Elsevier, Amsterdam, Vol. 6, pp. 427-437, https://doi.org/10.1016/j.egyr.2020.01.012

Energy Reports 6 (2020) 427–437

Contents lists available at ScienceDirect

Energy Reports

journal homepage: www.elsevier.com/locate/egyr

Research paper

Mitigation of Mismatch Power Losses of PV Array under Partial Shading Condition using novel Odd Even Configuration

Karan Yadav [a], Bhavnesh Kumar [b,*], Swaroop D. [b]

[a] Netaji Subhas Institute of Technology, New Delhi, India
[b] Netaji Subhas University of Technology, New Delhi, India

ARTICLE INFO

Article history:
Received 7 June 2019
Received in revised form 28 November 2019
Accepted 29 January 2020
Available online xxxx

Keywords:
Photovoltaic
Partial Shading Condition
Reconfiguration strategy
Global Maximum Power Point
Mismatch power loss

ABSTRACT

In this paper, the effect of Partial Shading Condition (PSC) on various solar photovoltaic (PV) array topologies has been studied extensively. PSC reduces the maximum power of a PV array and produces multiple Maximum Power Points (MPPs) in the PV characteristics. A novel PV array configuration, named as the Odd Even Configuration (OEC) has been proposed to mitigate the effects of PSC under a diagonally progressing shadowing scenario and performance parameters like mismatch power loss, Fill Factor (FF) and Performance Ratio (PR), have been measured. The performance of the proposed OEC has been compared with pre-existing standard configurations such as TCT, SP-TCT, BL-TCT and BL-HC. Another recently proposed configuration has also been used for comparison. The effect of variation in temperature on the shade dispersion effect has also been studied. All the considered PV array configurations have been modeled in MATLAB/Simulink environment. The proposed OEC configuration is found to be superior to other configurations for all the PSCs considered, with minimum power loss and improved FF.

1. Introduction

In the present scenario, the world is spiraling down into an energy crisis. Conventional energy resources like fossil fuels are being depleted at an alarming rate and may be completely exhausted in the next few decades. In a situation like this, it is only logical to look for an alternate source to meet our energy demands. A feasible alternative can be found in renewable energy resources, which offer easy availability and get replenished over time, so they would not be depleted. Though the renewable energy sources might be easily available, harnessing them to their full extent still remains a challenge. Some strides have been made in renewable energy technology, especially in the field of solar photovoltaic (PV) based power generation (Bishop, 1988).

Out of all the renewable energy generation technologies, solar PV energy is the most dominant technology, owing to availability of sunlight over wide geographical area and direct conversion of sunlight to electricity. In the year 2018, the total renewable energy generation capacity was at 2195 GW, which represents 18.2% of global human energy consumption. Of this, the solar PV energy generation capacity is at 402 GW which accounts for 1.73% of global energy generation (Ashouri-Zadeha et al., 2018).

One of the major challenges in tracking the Maximum Power Point (MPP) of a solar PV system is the occurrence of a Partial Shading Condition (PSC) (Kovach and Schmid, 1996). Under PSC, due to nearby objects, buildings, clouds etc., some of the modules of the PV array end up getting shaded, while the other modules receive the full insolation. This turns out to be problematic as not only does it reduce the maximum power of the PV array but also makes the P–V and I–V curves of the PV array extremely non-linear with multiple optima (MPPs), the greatest of which is referred to as the global maximum power point (GMPP) and all the other optima are referred to as local maximum power points (LMPPs) (Karatepe et al., 2007; Ashouri-Zadeha et al., 2018).

The effect of PSC can be remedied to some extent by using different interconnections within a solar PV array. This is achieved by connecting the PV modules within a PV array in ways other than the classic Series Parallel (SP) configuration. This provides some alternate paths for the current to flow, when some modules in a row are shaded and the current generated by them is reduced. A few of the configurations that can be obtained in this manner are Total Cross Tied (TCT), Series Parallel-Total Cross Tied (SP-TCT), Bridge Link-Total Cross Tied (BL-TCT) and Bridge Link-Honey Comb. SP, TCT, BL and HC configurations for 6 × 4 and 5 × 3 size PV arrays have been investigated in Villa et al. (2012) for different partial shading scenarios. For most of the practical cases of partial shadowing, TCT has been found to offer the best result out of all the configurations. Though, changing the connections

* Corresponding author.
E-mail addresses: karanyadav799@gmail.com (K. Yadav), kumar_bhavnesh@nsut.ac.in (B. Kumar), swaroopdevaraju@gmail.com (Swaroop D).

https://doi.org/10.1016/j.egyr.2020.01.012

can decrease the effect of partial shading, it can only be done to a limited extent (Quaschning and Hanitscht, 1996) (de Blas et al., 2002).

Another method of mitigating the effect of partial shading further is to disperse the shadow over the entire array as evenly as possible. Since, we cannot change the pattern of the shadow that is incident on the PV array, dispersion can be achieved by interchanging the positions of the PV modules within a PV array, while keeping their connections the same. Using this reconfiguration method, many such PV array configurations have been developed in the past. In Shams El-Dein et al. (2011), Half Reconfiguration Photovoltaic Array (HRPVA) and Full Reconfiguration Photovoltaic Array (FRPVA) have been investigated along with SP, TCT and BL configurations for 6 × 4 PV arrays under different shading scenarios. The best results are obtained with the use of HRPVA configuration. A reconfiguration pattern for 9 × 9 size PV array based on the Su-Do-Ku puzzle has been proposed in Indu Rani et al. (2013) and has been shown to offer better performance than conventional configurations under PSCs. An optimization based approach to change the connections between the PV modules while keeping their physical locations fixed has been analyzed in Malathy and Ramaprabha (2015) and Deshkar et al. (2015). Further, a shadow dispersion technique utilizing GA based optimization technique for Su-Do-Ku PV array configuration has been proposed which offers minimum power loss and best FF.

In Potnuru et al. (2015) and Vijayalekshmy et al. (2015), Reconfiguration TCT (RTCT) configuration has been compared and found to be superior to TCT by investigating power losses and FF. A magic-square puzzle configuration has been proposed and found to be superior to other configurations for 4 × 4 PV array in Yadav et al. (2017). In Vijayalekshmy et al. (2016) a new configuration has been proposed with Zig-Zag technique has been proposed to modify the connections of TCT configuration in order to reduce power losses and improve FF. A novel 6 × 4 PV array configuration that can be applied to any $m \times n$ configuration has been proposed in Mishra et al. (2017) and found to offer superior performance to conventional configurations in most of the cases. In this paper, a novel configuration, named the Odd Even Configuration (OEC), has been proposed and compared with other configurations such as TCT, SP-TCT, BL-TCT, BL-HC and the novel configuration proposed in Mishra et al. (2017) and it has been shown to offer the best performance under all the PSCs considered.

The main objective of this paper is to present a method so as to mitigate the effects arising due to the occurrence of a partial shading condition, by reconfiguring the physical positions of the PV modules within a TCT connected PV array. The modules have been reconfigured in an Odd Even pattern, where all the odd numbered modules are positioned together and even numbered modules are also positioned together.

The following discussions in this paper are segregated as follows: Section 2 explains the mathematical models used to simulate the behavior of PV systems. Section 3 describes the various 6 × 4 PV array configurations that are used to compare the performance of the proposed method. Section 4 describes the proposed reconfiguration method of OEC and provides the mathematical formulation for the same. In Section 5, the partial shading cases considered for the diagonally progressing shadow movements are explained and analyzed. Results and discussions are presented in Section 6. Finally, the conclusions of the detailed analysis are summarized in Section 7.

2. Mathematical Modeling of PV Sytem

To study the effects due to Partial Shading Conditions (PSCs), and their mitigation, on solar PV systems, a mathematical model of the solar PV array has been developed in MATLAB/Simulink environment. First, a model for a single PV module is developed and then multiple such modules are interconnected in different configurations to construct a solar PV array.

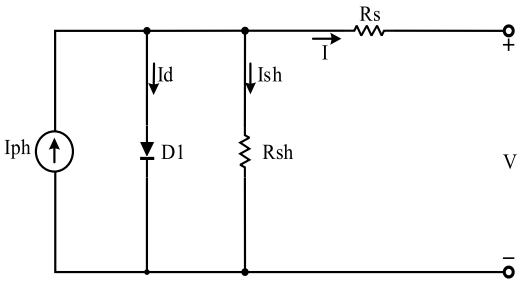

Fig. 1. Equivalent circuit model of a solar PV module.

2.1. Mathematical model of PV module

The equivalent circuit model of a solar PV module has been illustrated in Fig. 1. Using this equivalent circuit, a mathematical model is developed for a single PV module.

The equivalent circuit of a solar module consists of a photo generated current source connected in parallel with a p–n junction diode, D_1. To account for the combined internal resistances of the solar PV cells in the module, a resistance, R_{sh}, called the shunt resistance, is connected in parallel with the diode and current source. Similarly, another resistance, R_s, known as the series resistance, is connected in series with the diode, just before the output terminals.

The photo current, I_{ph}, that is generated by the PV module, due to the incidence of solar irradiation on its surface, depends on both the insolation received and the temperature of solar PV module surface, and can be expressed in Eq. (1) as:

$$I_{ph} = (I_{sc} + k_i(T - T_n))\frac{G}{G_o} \tag{1}$$

This photo current is then divided into three paths, and by applying KCL at the junction can be expressed in Eq. (2) as:

$$I_{ph} = I_d + I_{sh} + I \tag{2}$$

The current that flows through the diode, I_d, can be expressed using the Shockley diode equation in Eq. (3) as:

$$I_d = I_o\left(e^{(V+IR_s)/nV_T} - 1\right) \tag{3}$$

where the current, I_o, can further be expanded in Eq. (4) as:

$$I_o = I_{rs}\left(\frac{T}{T_n}\right)^3 e\left(\frac{qE_{go}\,(1/T_n - 1/T)}{nk_B}\right) \tag{4}$$

where the reverse saturation current, I_{rs}, can be expressed in Eq. (5) as:

$$I_{rs} = \frac{I_{sc}}{\left(e^{\left(\frac{qV_{OC}}{nk_BT}\right)} - 1\right)} \tag{5}$$

Using the above equations, Eq. (2) can be rewritten and rearranged to express the output terminal current, I, in Eq. (6) as:

$$I = I_{ph} - I_o(e^{(V+IR_s)/nV_T} - 1) - \frac{(V + IR_s)}{R_{sh}} \tag{6}$$

Rearranging the terms in the above equations, the output terminal voltage, V, can be expressed in Eq. (7) as:

$$V = nV_T \ln\left(\frac{I_{ph} + I_o - I}{I_o}\right) - IR_s \tag{7}$$

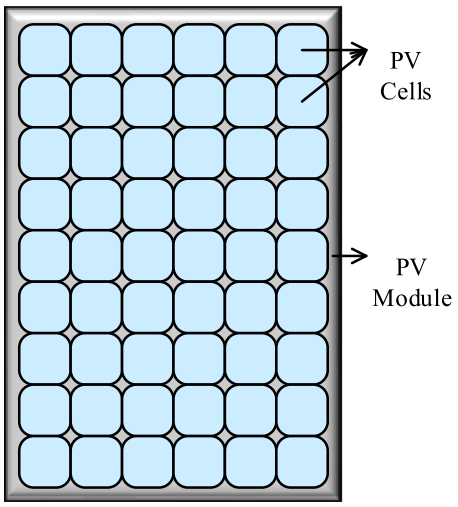

Fig. 2. A solar PV module of 54 PV cells connected in series.

Table 1
Parameters of solar PV module KC200GT at STC (1000 W/m^2 and 25°C).

Parameters of PV module	
Parameter	Value
Maximum power of the module , P_{max}	200 W
Open circuit voltage, V_{oc}	32.9 V
Short circuit current, I_{sc}	8.21 A
Voltage at MPP, V_{mpp}	26.4 V
Current at MPP, I_{mpp}	7.58 A
Temperature coefficient of current, k_i	0.0032 A/°C
No. of cells connected in parallel, N_p	1
No. of cells connected in series, N_s	54

A solar PV module consists of a number of PV cells that are connected to each other in series and parallel combinations as depicted in Fig. 2. Here, a PV module with 54 solar PV cells connected in series has been selected.

In this paper, a model is generated for a solar PV module using the above equations in MATLAB Simulink. The characteristics of the module are based on the commercially available KC200GT module and have been tabulated in Table 1.

2.2. Mathematical model of PV array

In order to supply power to loads greater than the maximum power output of a single solar PV module, a number of such modules are connected together in various combinations of series and parallel. A bypass diode is connected in anti-parallel with each module to bypass it, in case of mismatch in generated current within a series string.

If there are N_s number of modules connected in series, then the output voltage of the PV array will be equal to N_s times the voltage of a single PV module. Similarly, if N_P number of modules are connected in parallel, then the output current of the PV array will be equal to N_p times the current of a single PV module.

The voltage and current equations for a solar PV array consisting of $N_s \times N_p$ modules, can then be rewritten in Eq. (8) as:

$$\left.\begin{aligned} V_{pv} &= N_s V \\ I_{pv} &= N_p I \\ V_{oc} &= N_s V_{oc_m} \\ I_{sc} &= N_p I_{sc_m} \\ R_{s_A} &= \left(N_s/N_p\right) R_s \end{aligned}\right\} \tag{8}$$

The expression for output voltage and output current of the photovoltaic array can then be modified and rewritten in Eq. (9) as:

$$V_{pv} = nV_T \ln\left(\frac{I_{ph_A} + I_{o_A} - I_{pv}}{I_{o_A}}\right) - I_{pv}R_{s_A} \tag{9}$$

In this paper, we have used a 6 × 4 PV array in different configurations as discussed in the next section.

3. Description of various 6 × 4 PV array configurations used

To investigate the effectiveness of the proposed Odd Even Configuration of PV array in mitigating the effect of a diagonally progressing partial shadow, it has to be compared with some pre-existing standard configurations. Four such configurations, namely, the Total Cross Tied (TCT), Series Parallel-TCT (SP-TCT), Bridge Link-TCT (BL-TCT) and Bridge Link-Honey Comb (BL-HC) have been modeled in MATLAB/Simulink and used for comparing the P–V and I–V characteristics of the OE configuration under various partial shading conditions. A comparison has also been made with another reconfiguration technique proposed in Mishra et al. (2017), hereafter referred to as ASY configuration. All these PV array configurations are depicted in Fig. 3.

In TCT configuration, PV modules are connected in a series connection in groups of six, giving rise to four such series strings which are connected in parallel, similar to a standard Series Parallel (SP) configuration. In addition to this, series strings are interconnected in parallel at the end of every row as well, as can be seen from Fig. 3(a). SP-TCT configuration is hybrid of SP and TCT configurations, in which the modules in two adjacent series strings are interconnected at the end of every other row (connected in an alternate pattern) as shown in Fig. 3(b). Similarly, BL-TCT and BL-HC configurations have been modeled by connecting the PV modules in the manner depicted in Fig. 3(c) and (d), respectively. BL-TCT is similar to SP-TCT, the difference being that some of the modules that were left unconnected in SP-TCT in alternate rows are now connected through a bridge, but the entire row is not connected as in TCT. BL-HC follows the same logic as BL-TCT but the interconnections are now made according to a pattern that resembles the structure of a honey comb.

In ASY configuration, the PV modules are connected in exactly the same manner as TCT configuration, but the physical positions of the modules within the PV array are interchanged according to a puzzle pattern and depicted in Fig. 3(e).

4. Proposed Odd Even Configuration

In this paper, a novel configuration, named the Odd Even Configuration (OEC), is presented as depicted in Fig. 4. The electrical connections between the PV modules, like the ASY configuration, are made in a manner which is exactly the same as TCT configuration. But within a series column string, all the PV modules belonging to an odd numbered row according to their electrical connection, are clumped together physically within a PV array. After placing all the odd numbered modules in this manner within a column, they are followed by modules belonging to even numbered rows according the electrical connections, which are again clumped together. Furthermore, the physical position of the module connected in the 1st row of a given column is shifted by a certain number of rows after every column in arithmetic position.

For an $m \times n$ PV array, the row index (physical position) of a module which is electrically connected in the ith and jth is determined by the following method.

For a module, which is connected in the 1st row of any given column, its row index can be expressed as:

$$R_{1j} = 1 + (j-1)\,2 \tag{10}$$

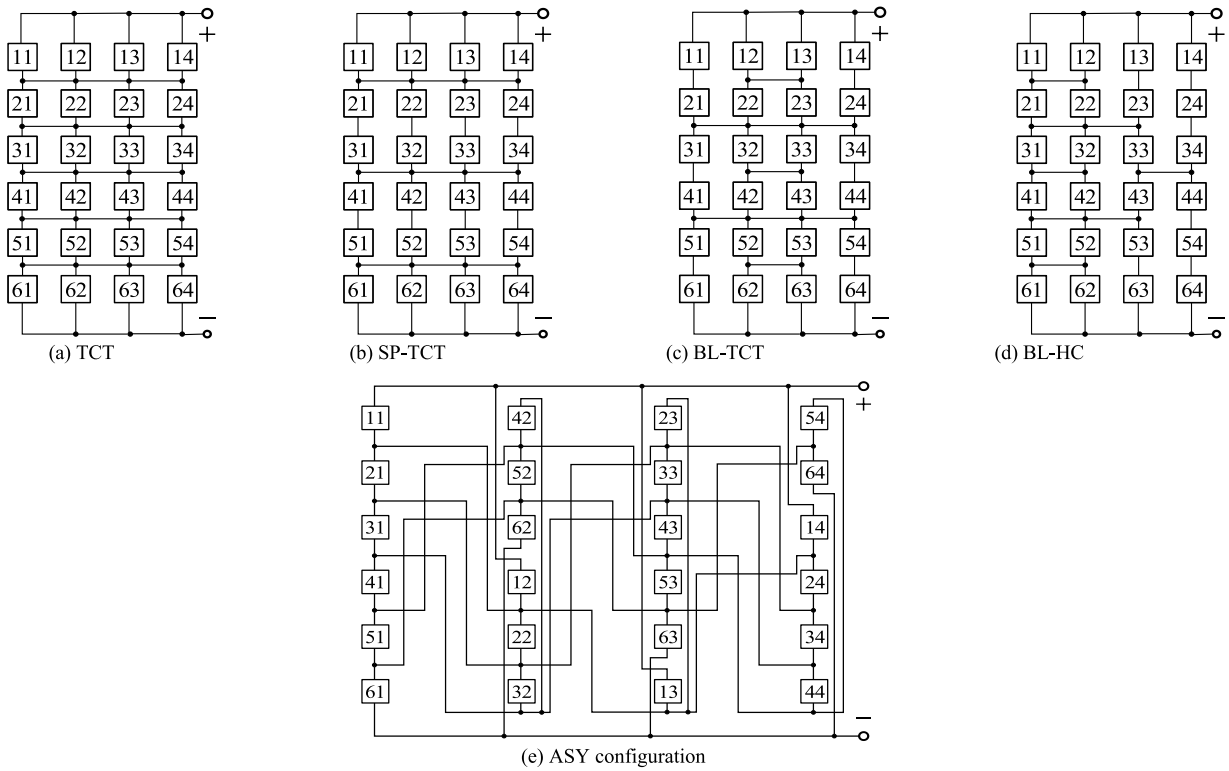

Fig. 3. Interconnection of PV modules within an array for the various PV array configurations used for comparison.

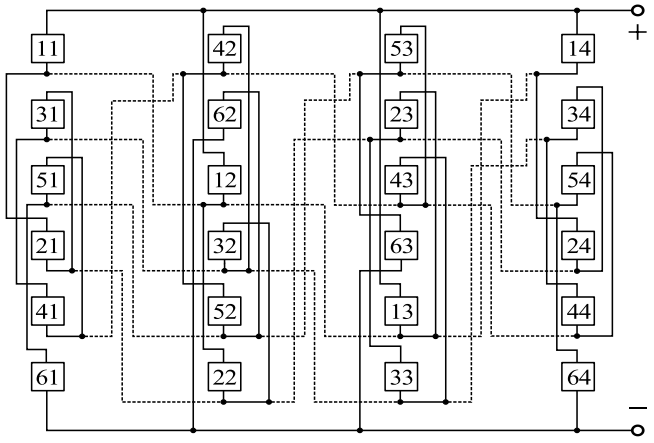

Fig. 4. The interconnections of PV modules within a 6 × 4 PV array with OEC.

For all the other modules electrically connected in an odd numbered of rows,

$$R_{ij} = R_{1j} + (i-1)/2 \tag{11}$$

For all the other modules electrically connected in an even numbered of rows,

$$R_{ij} = R_{1j} + m/2 + i/2 - 1 \tag{12}$$

5. Analysis of various partial shading conditions considered

5.1. Analysis of diagonally progressing shadow at STC

Partial Shading Condition refers to the case when some of the PV modules of the PV array end up getting shaded, due to the presence of some nearby object, building, tree, clouds etc., while other modules of the array receive the full insolation of the sun. Due to this, a mismatch is created between the current flowing in the rows of the PV array. As a result, multiple peaks are present in the P–V characteristics of the PV array and the maximum power that can be extracted from the PV array gets reduced due to the mismatch power loss.

Here, four different partial shading scenarios have been considered for a diagonally progressing shadow movement, as depicted in Fig. 5. The diagonal shadow starts at the lower left corner of the 6 × 4 PV array, shading only 3 modules in case 5(a) and progresses upwards and rightwards to the upper right corner, shading up to 12 PV modules in the process in case 5(d).

As can be seen from Fig. 5(a), for case 5(a), the PV modules in rows 1, 2 and 3, all receive the full 1000 W/m^2 insolation of the sun, while three of the modules in each of the rows 4, 5 and 6 receive the full solar insolation of 1000 W/m^2 and one module receives a reduced insolation of 350 W/m^2.

So, for case 5(a), the currents generated in the 1st, 2nd and 3rd rows for TCT configuration can be expressed in Eq. (13) as:

$$I_{R_1} = I_{R_2} = I_{R_3} = 4I \tag{13}$$

And, the currents generated in the 4th, 5th and 6th rows for TCT configurations can be expressed in Eq. (14) as:

$$I_{R_4} = I_{R_5} = I_{R_6} = 3.35I \tag{14}$$

Similarly, the currents circulating in the rows of the PV array can be formulated as follows from Eqs. (15) to (17).

For Case 5(b):

$$\left.\begin{aligned} I_{R_1} &= I_{R_2} = 4I \\ I_{R_3} &= I_{R_6} = 3.35I \\ I_{R_4} &= I_{R_5} = 2.7I \end{aligned}\right\} \tag{15}$$

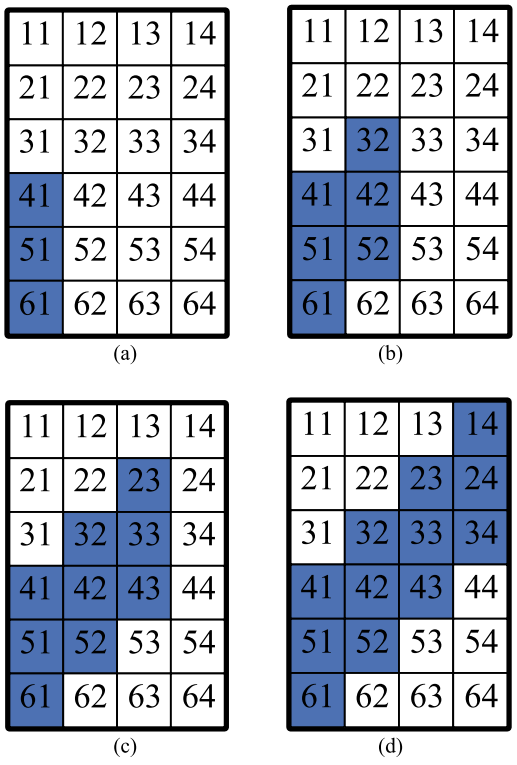

Fig. 5. Diagonal shading cases considered for various 6 × 4 PV array configurations.

For case 5(c):

$$\left.\begin{aligned} I_{R_1} &= 4I \\ I_{R_2} &= I_{R_6} = 3.35I \\ I_{R_3} &= I_{R_5} = 2.7I \\ I_{R_4} &= 2.05I \end{aligned}\right\} \tag{16}$$

For case 5(d):

$$\left.\begin{aligned} I_{R_1} &= I_{R_6} = 3.35I \\ I_{R_2} &= I_{R_5} = 2.7I \\ I_{R_3} &= I_{R_4} = 2.05I \end{aligned}\right\} \tag{17}$$

For ASY configuration, same shading pattern is applied to the puzzle configuration and the modules are then rearranged within the PV array to analyze the electrical effect of dispersion of shadow, as depicted in Fig. 6. So, for case 5(a), the currents generated in the 1st, 2nd and 3rd rows for ASY configuration can be expressed in Eq. (18) as:

$$I_{R_1} = I_{R_2} = I_{R_3} = 4I \tag{18}$$

And, the currents generated in the 4th, 5th and 6th rows for ASY configurations can be expressed in Eq. (19) as:

$$I_{R_4} = I_{R_5} = I_{R_6} = 3.35I \tag{19}$$

Similarly, the currents generated for shading case 5(b), for ASY configuration are expressed from Eqs. (20) to (22) as:

$$\left.\begin{aligned} I_{R_1} &= I_{R_2} = I_{R_4} = I_{R_5} = 3.35I \\ I_{R_3} &= 4I \\ I_{R_6} &= 2.7I \end{aligned}\right\} \tag{20}$$

For case 5(c):

$$\left.\begin{aligned} I_{R_1} &= I_{R_2} = I_{R_3} = 3.35I \\ I_{R_4} &= I_{R_5} = I_{R_6} = 2.7I \end{aligned}\right\} \tag{21}$$

For case 5(d):

$$\left.\begin{aligned} I_{R_1} &= I_{R_4} = 2.7I \\ I_{R_2} &= I_{R_3} = 3.35I \\ I_{R_5} &= I_{R_6} = 2.05I \end{aligned}\right\} \tag{22}$$

For OEC configuration same shading pattern is again applied to the OEC and rearrangement of the modules is done to analyze the electrical effect of dispersion of shadow, as can be seen in Fig. 7. So, for case 5(a), the currents generated in the 1st, 3rd and 5th rows for OEC can be expressed in Eq. (23) as:

$$I_{R_1} = I_{R_3} = I_{R_5} = 4I \tag{23}$$

the currents generated in the 2nd, 4th and 6th rows for OEC can be expressed in Eq. (24) as:

$$I_{R_2} = I_{R_4} = I_{R_6} = 3.35I \tag{24}$$

For case 5(b), the shadow is dispersed in such a way that each row has one shaded module receiving 350 W/m^2 of solar insolation and three unshaded modules receiving the full 1000 W/m^2 of solar insolation, as depicted in Fig. 7(b). So, the currents generated in all the rows are expressed from Eqs. (25) to (27) as:

$$I_{R_1} = I_{R_2} = I_{R_3} = I_{R_4} = I_{R_5} = I_{R_6} = 3.35I \tag{25}$$

Similarly, for case 5(c):

$$\left.\begin{aligned} I_{R_1} &= I_{R_3} = I_{R_5} = 3.35I \\ I_{R_2} &= I_{R_4} = I_{R_6} = 2.7I \end{aligned}\right\} \tag{26}$$

For case 5(d):

$$I_{R_1} = I_{R_2} = I_{R_3} = I_{R_4} = I_{R_5} = I_{R_6} = 2.7I \tag{27}$$

5.2. Analysis of diagonally progressing shadow movements and effect of shade dispersion at variable temperature

The operation of OEC and ASY configurations under the diagonally progressing partial shadow movements discussed above (cases 5(a)–5(d)), at different temperature levels of T = 20 °C and T = 15 °C, has been considered. The effects of temperature on the currents generated in the different rows of the two PV array configurations have been analyzed.

For case 5(a) with a temperature of T = 20 °C at shaded modules, the currents generated in the 1st, 2nd and 3rd rows for ASY configuration can be expressed in Eq. (28) as:

$$I_{R_1} = I_{R_2} = I_{R_3} = 4I \tag{28}$$

And, the currents generated in the 4th, 5th and 6th rows for ASY configurations can be expressed in Eq. (29) as:

$$I_{R_4} = I_{R_5} = I_{R_6} = 3.35I + 0.0056 \tag{29}$$

Similarly, for case 5(b):

$$\left.\begin{aligned} I_{R_1} &= I_{R_2} = I_{R_4} = I_{R_5} = 3.35I + 0.0056 \\ I_{R_3} &= 4I \\ I_{R_6} &= 2.7I + 0.0112 \end{aligned}\right\} \tag{30}$$

For case 5(c):

$$\left.\begin{aligned} I_{R_1} &= I_{R_2} = I_{R_3} = 3.35I + 0.0056 \\ I_{R_4} &= I_{R_5} = I_{R_6} = 2.7I + 0.0112 \end{aligned}\right\} \tag{31}$$

For case 5(d):

$$\left.\begin{aligned} I_{R_1} &= I_{R_4} = 2.7I + 0.0112 \\ I_{R_2} &= I_{R_3} = 3.35I + 0.0056 \\ I_{R_5} &= I_{R_6} = 2.05I + 0.0168 \end{aligned}\right\} \tag{32}$$

Similarly, the row-wise currents generated in OEC when shaded modules are at a temperature of T = 20 °C are described below.

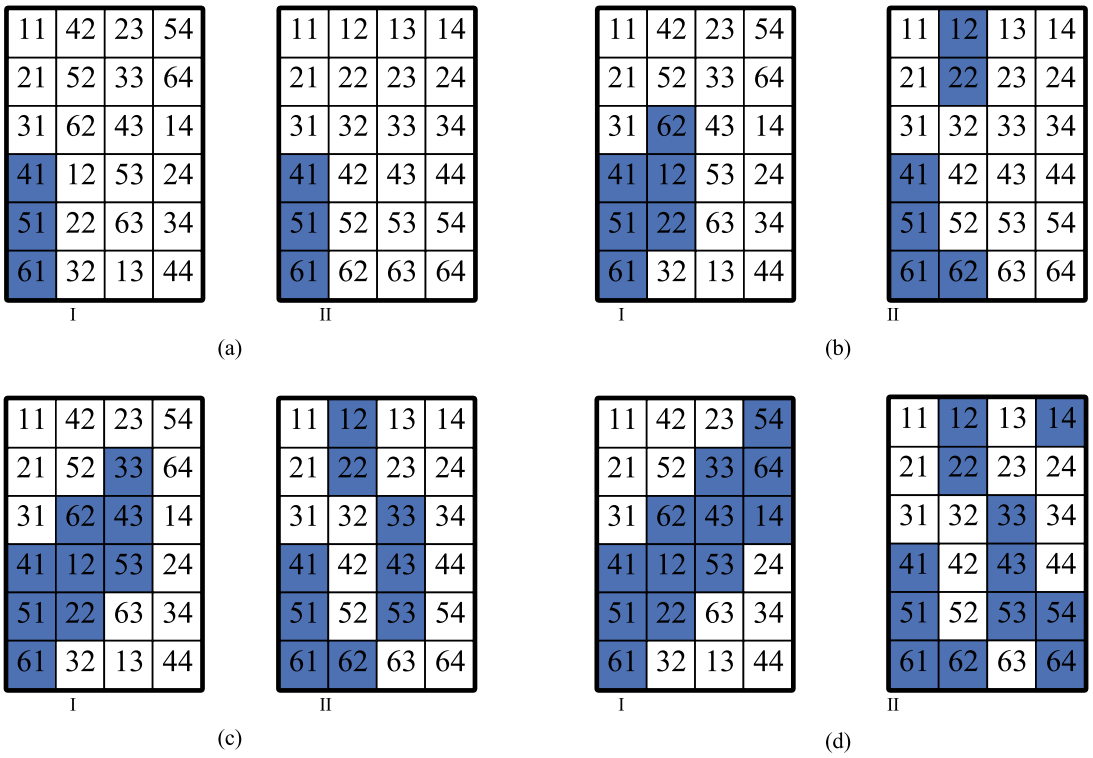

Fig. 6. Diagonally progressing PSCs considered for 6 × 4 ASY configuration and the effect of shade dispersion due to reconfiguration. Part I of each figure shows how the shadow is incident on the PV array and Part II shows how the effect is distributed over the entire array electrically.

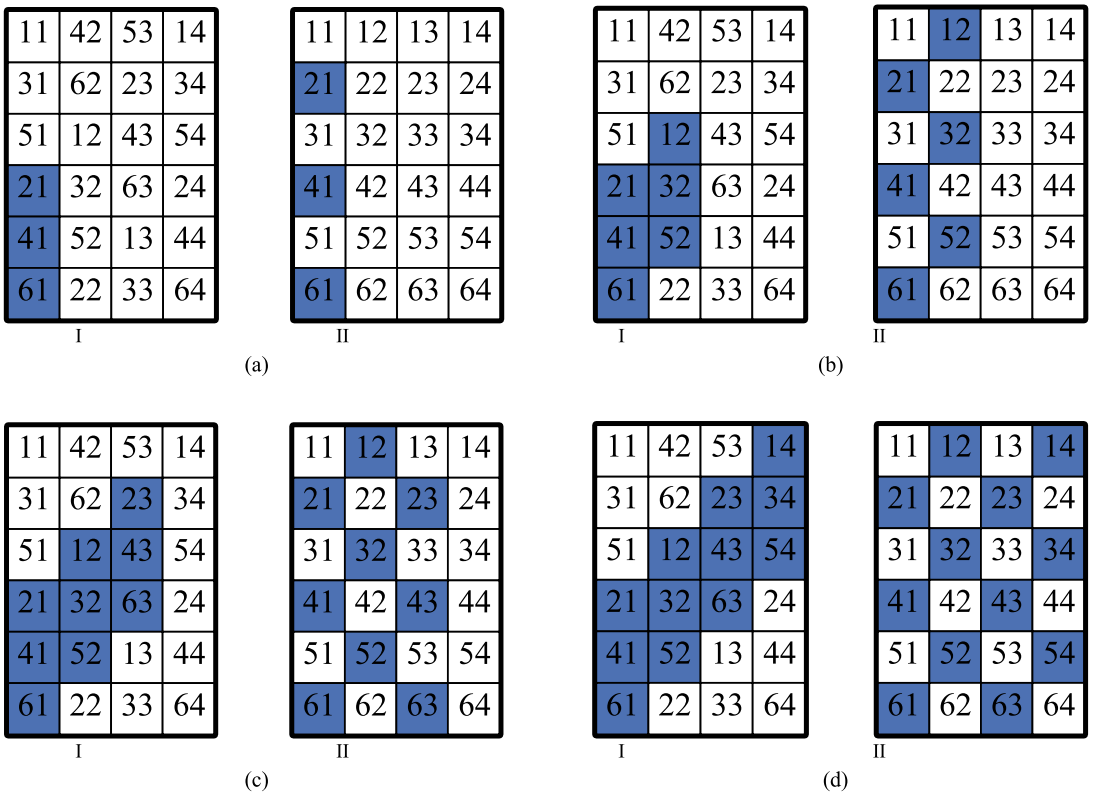

Fig. 7. Diagonally progressing PSCs considered for 6 × 4 OEC connected PV array and the effect of shade dispersion due to reconfiguration. Part I of each figure shows how the shadow is incident on the PV array and Part II shows how the effect is distributed over the entire array electrically.

For case 5(a), the currents generated in the 1st, 3rd and 5th rows for OEC can be expressed in Eq. (33) as:

$$I_{R_1} = I_{R_3} = I_{R_5} = 4I \tag{33}$$

And, the currents generated in the 2nd, 4th and 6th rows for OEC can be expressed in Eq. (34) as:

$$I_{R_2} = I_{R_4} = I_{R_6} = 3.35I + 0.0056 \tag{34}$$

For case 5(b):

$$I_{R_1} = I_{R_2} = I_{R_3} = I_{R_4} = I_{R_5} = I_{R_6} = 3.35I + 0.0056 \tag{35}$$

For case 5(c):

$$\left.\begin{aligned} I_{R_1} = I_{R_3} = I_{R_5} &= 3.35I + 0.0056 \\ I_{R_2} = I_{R_4} = I_{R_6} &= 2.7I + 0.0112 \end{aligned}\right\} \tag{36}$$

For case 5(d):

$$I_{R_1} = I_{R_2} = I_{R_3} = I_{R_4} = I_{R_5} = I_{R_6} = 2.7I + 0.0112 \tag{37}$$

Another case with a temperature of T = 15 °C at shaded modules has been considered and for case 5(a) the currents generated in the 1st, 2nd and 3rd rows for ASY configuration can be expressed in Eq. (38) as:

$$I_{R_1} = I_{R_2} = I_{R_3} = 4I \tag{38}$$

And, the currents generated in the 4th, 5th and 6th rows for ASY configurations can be expressed in Eq. (39) as:

$$I_{R_4} = I_{R_5} = I_{R_6} = 3.35I + 0.0112 \tag{39}$$

Similarly, for case 5(b):

$$\left.\begin{aligned} I_{R_1} = I_{R_2} = I_{R_4} = I_{R_5} &= 3.35I + 0.0112 \\ I_{R_3} &= 4I \\ I_{R_6} &= 2.7I + 0.0224 \end{aligned}\right\} \tag{40}$$

For case 5(c):

$$\left.\begin{aligned} I_{R_1} = I_{R_2} = I_{R_3} &= 3.35I + 0.0112 \\ I_{R_4} = I_{R_5} = I_{R_6} &= 2.7I + 0.0224 \end{aligned}\right\} \tag{41}$$

For case 5(d):

$$\left.\begin{aligned} I_{R_1} = I_{R_4} &= 2.7I + 0.0224 \\ I_{R_2} = I_{R_3} &= 3.35I + 0.0112 \\ I_{R_5} = I_{R_6} &= 2.05I + 0.0336 \end{aligned}\right\} \tag{42}$$

For OEC, at T = 15 °C, the currents generated in the 1st, 3rd and 5th rows for case 5(a) can be expressed in Eq. (43) as:

$$I_{R_1} = I_{R_3} = I_{R_5} = 4I \tag{43}$$

And, the currents generated in the 2nd, 4th and 6th rows for OEC can be expressed in Eq. (44) as:

$$I_{R_2} = I_{R_4} = I_{R_6} = 3.35I + 0.0112 \tag{44}$$

For case 5(b):

$$I_{R_1} = I_{R_2} = I_{R_3} = I_{R_4} = I_{R_5} = I_{R_6} = 3.35I + 0.0112 \tag{45}$$

For case 5(c):

$$\left.\begin{aligned} I_{R_1} = I_{R_3} = I_{R_5} &= 3.35I + 0.0112 \\ I_{R_2} = I_{R_4} = I_{R_6} &= 2.7I + 0.0224 \end{aligned}\right\} \tag{46}$$

For case 5(d):

$$I_{R_1} = I_{R_2} = I_{R_3} = I_{R_4} = I_{R_5} = I_{R_6} = 2.7I + 0.0112 \tag{47}$$

Table 2
Performance characteristics of various PV array configurations for case 5(a).

PV array configuration	Case 5(a)				
	GMPP	V_m	Power loss	FF	%PR
TCT	4219	161.2	581	0.6553	87.90
SP-TCT	4219	161.2	581	0.6553	87.90
BL-TCT	4154	160.4	646	0.6452	86.54
BL-HC	4162	161.4	638	0.6464	86.71
ASY	4219	161.2	581	0.6553	87.90
OEC	4219	161.2	581	0.6553	87.90
Best configuraion	TCT/SP-TCT/ASY/OEC				

6. Results and discussions

6.1. P-V characteristics for diagonal shading at STC

The P–V characteristics of all the configurations of PV array considered for diagonal shading cases 5(a)–5(d) are depicted and compared in Fig. 8. From Fig. 8(a), it is observed that two MPPs are present in the P–V curves of all the configurations. The LMPP is found to be at a distance from the GMPP and might increase the effect of partial shading. The GMPP for OEC, TCT, SP-TCT and ASY configurations is found to be 4219 W and is a true GMPP for PSC of case 5(a). The maximum power of the remaining configurations of BL-TCT and BL-HC are found to be 4154 W and 4162 W respectively and are fairly close to true GMPP.

Fig. 8(b), considers the shading condition of case 5(b). For OEC, a single MPP is observed at 3999 W and is a true GMPP for shadow condition of case 5(b). For ASY configuration, two MPPs are observed and maximum power is found to be 3607 W, which is at a distance from true GMPP and increases the effect of shading. Three MPPs are observed for the remaining configurations of TCT, SP-TCT, BL-TCT and BL-HC with a maximum power of 3530 W, 3517 W, 3430 W and 3372 W respectively.

The P–V curves for diagonal shadowing condition of case 5(c) are depicted in Fig. 8(c). OEC and ASY configurations have identical curves, with two MPPs and the maximum power is found to be 3396 W and is a true GMPP for PSC of case 5(c). The LMPP is at a distance from the GMPP and might increase the effect of shading. For the other configurations of TCT, SP-TCT, BL-TCT and BL-HC, four MPPs are observed and their maximum powers are found to be 2878 W, 2864 W, 2889 W and 2914 W respectively, which are at a distance from the true GMPP.

The P–V curves for the diagonal shadowing condition of case 5(d) are depicted in Fig. 8(d). For OEC, a single maximum power point is observed at 3198 W and is a true GMPP for shadow condition of case 5(d). For all the other configurations three MPPs at different locations are observed and the maximum power for TCT, SP-TCT, BL-TCT, BL-HC and ASY are found to be 2680 W, 2572 W, 2746 W, 2711 W and 2680 W respectively, which are at a distance from the true GMPP and increase the effect of shading.

The performance of all the considered PV configurations are compared for the partial shading conditions of case 5(a)–5(d) in Tables 2–5, in terms maximum power, voltage at which MPP occurs, power losses, fill factor and performance ratio.

6.2. Power losses and FF for diagonal shading at STC

The power losses and fill factor of the various PV array configurations are shown as bar graphs in Fig. 9 and they have been tabulated along with performance ratio in Tables 2–5.

It is observed that for case 5(a), power loss and FF of OEC are the same as that of TCT and ASY configurations and for case 5(c), power loss and FF are the same as that of ASY configuration. For shadowing condition of case 5(b), the power loss for OEC is 392

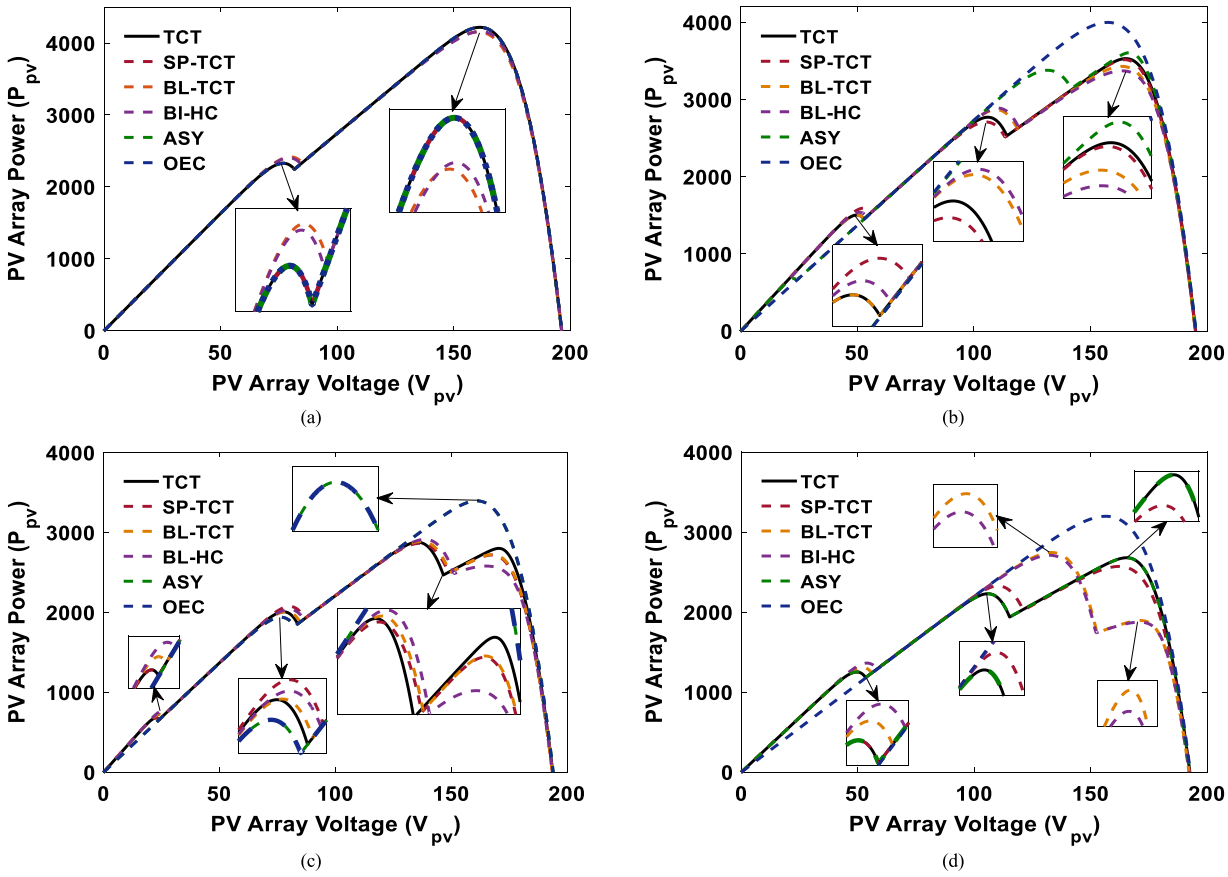

Fig. 8. P–V characteristics of various 6 × 4 PV array configurations studied for diagonally progressing shadow movements considered in Case 5(a)–5(b), at STC, obtained using MATLAB/Simulink.

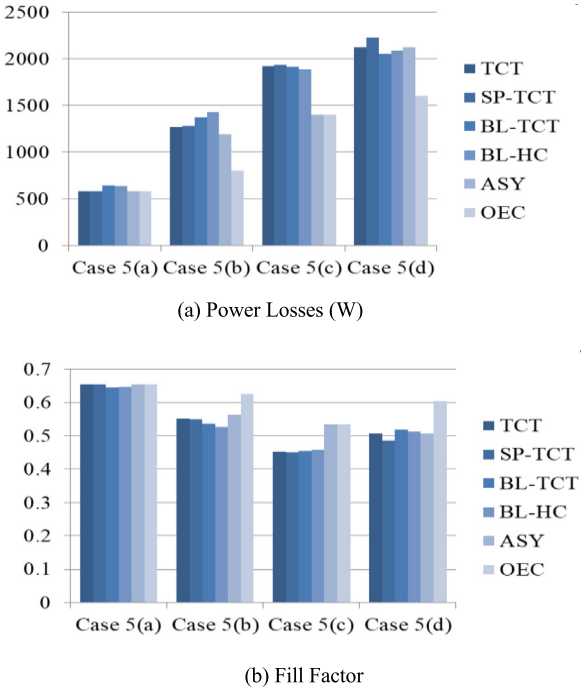

Fig. 9. Power losses and fill factor of various PV array configurations.

Table 3
Performance characteristics of various PV array configurations for case 5(b).

PV array configuration	Case 5(b)				
	GMPP	V_m	Power loss	FF	%PR
TCT	3530	165.1	1270	0.5513	73.54
SP-TCT	3517	164.6	1283	0.5493	73.27
BL-TCT	3430	163.4	1370	0.5357	71.46
BL-HC	3372	163.6	1428	0.5267	70.25
ASY	3607	166.6	1193	0.5634	75.15
OEC	3999	157.4	801	0.6246	83.31
Best configuraion		OEC			

Table 4
Performance characteristics of various PV array configurations for case 5(c).

PV array configuration	Case 5(c)				
	GMPP	V_m	Power loss	FF	%PR
TCT	2878	135.4	1922	0.4528	59.96
SP-TCT	2864	136.4	1936	0.4506	59.67
BL-TCT	2889	137.2	1911	0.4545	60.19
BL-HC	2914	138.6	1886	0.4584	60.71
ASY	3396	161	1404	0.5342	70.75
OEC	3396	161	1404	0.5342	70.75
Best configuraion		ASY/OEC			

W less than ASY configuration and FF is 10.86% more than ASY configuration. For shadowing condition of case 5(d), the power loss for OEC is 452 W less that BL-TCT configuration and FF is 16.46% more than BL-TCT configuration.

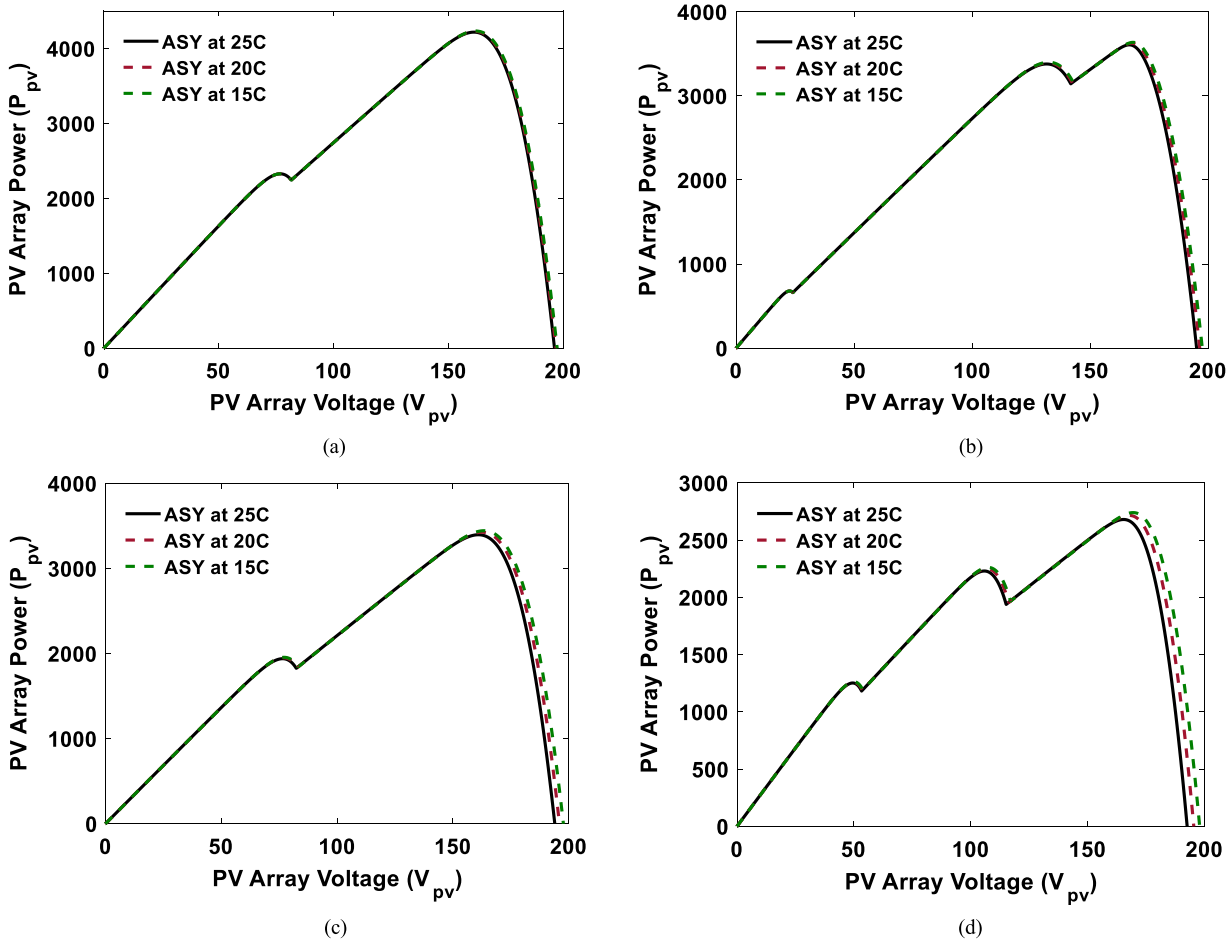

Fig. 10. P–V characteristics of 6 × 4 ASY configuration for diagonally progressing shadow movements considered in Case 5(a)–5(b), at variable temperature, obtained using MATLAB/Simulink.

Table 5
Performance characteristics of various PV array configurations for case 5(d).

PV array configuration	Case 5(d)				
	GMPP	V_m	Power loss	FF	%PR
TCT	2680	165.4	2120	0.5060	55.83
SP-TCT	2572	162.2	2228	0.4856	53.58
BL-TCT	2746	133.2	2054	0.5185	57.21
BL-HC	2711	132.2	2089	0.5118	56.48
ASY	2680	165.4	2120	0.5060	55.83
OEC	3198	156.5	1602	0.6038	66.62
Best configuraion		OEC			

6.3. Performance ratio of PV array configurations

The performance ratios of various PV array configurations are shown as bar graph in Fig. 12 and tabulated in Tables 2–5. In cases 5(b) and 5(d), the PR is increased from 75.15% in ASY configuration to 83.31% in OEC and from 57.21% in BL-TCT configuration to 66.62% in OEC respectively. Furthermore, OEC has the same response as TCT, SP-TCT and ASY configurations with a PR of 87.9% for case 5(a) and the same response as ASY configuration with a PR of 70.5% for case 5(c).

6.4. Effect of diagonal shading on P–V and I–V characteristics at variable temperature

The effect of temperature on the PV characteristics of ASY and OEC PV array configurations has been depicted in Figs. 10–11.

Table 6
Effect of variable temperature on ASY configuration.

Partial shading condition	ASY configuration		
	$T = 25$ °C	$T = 20$ °C	$T = 15$ °C
Case 5(a)	4219	4229	4234
Case 5(b)	3607	3626	3637
Case 5(c)	3396	3425	3443
Case 5(d)	2680	2716	2740

Three different temperature levels at T = 25 °C, T = 20 °C and T = 15 °C for the shaded modules of the diagonally progressing shadow cases of Fig. 5(a)–(d) have been considered. It has been observed that a decrease in the temperature of the PV modules, results into an increase in the maximum power available from the PV array (GMPP of the PV array).

For the partial shadowing cases 5(a) and 5(c), the performance characteristics of OEC are the same as that of ASY configuration. For case 5(b), the maximum power of OEC is 392 W, 394 W and 395 W more than that of ASY configuration at 25 °C, 20 °C and 15 °C respectively.

Similarly, for the partial shadowing case 5(d), the maximum power of OEC is 518 W, 523 W and 524 W more than that of ASY configuration at 25 °C, 20 °C and 15 °C respectively. The effect of temperature on the GMPP of OEC and ASY configuration for the diagonally progressing shadow movements has been tabulated in Tables 6–7.

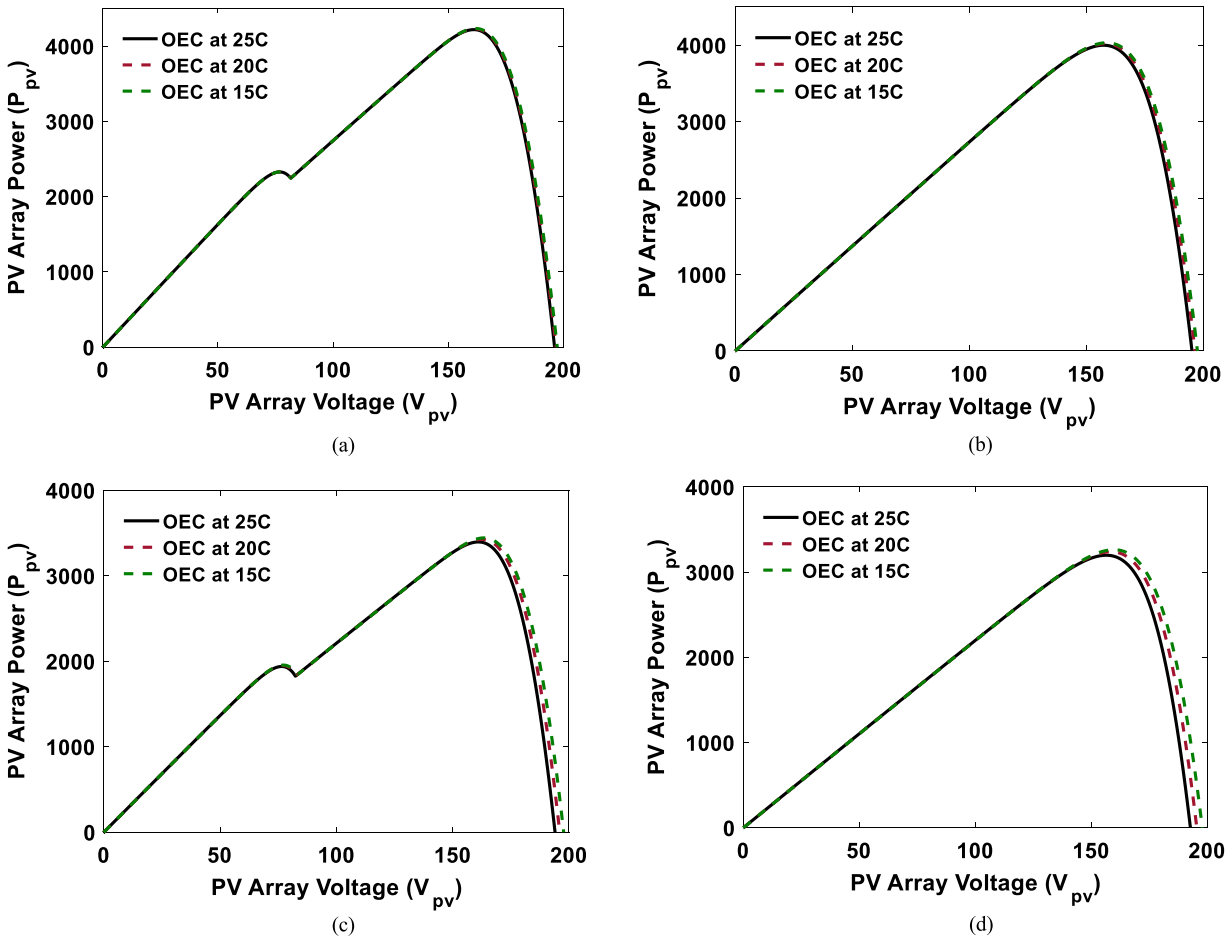

Fig. 11. P–V characteristics of 6 × 4 OEC connected PV array for diagonally progressing shadow movements considered in Case 5(a)–5(b), at variable temperature, obtained using MATLAB/Simulink.

Table 7
Effect of variable temperature on OEC.

Partial shading condition	OEC		
	$T = 25$ °C	$T = 20$ °C	$T = 15$ °C
Case 5(a)	4219	4229	4234
Case 5(b)	3999	4020	4032
Case 5(c)	3396	3425	3443
Case 5(d)	3198	3239	3264

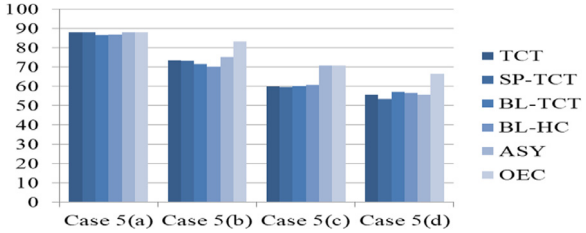

Fig. 12. Performance ratio of various PV array configurations.

7. Conclusion

Different PV array configurations, namely TCT, SP-TCT, BL-TCT, BL-HC, ASY and proposed novel configuration, OEC, have been extensively studied and analyzed. Various PSCs pertaining to a diagonally progressing shadow movements have been applied to the above configurations and the obtained parameters like maximum power, voltage, current, mismatch power loss, fill factor and % performance ratio have been used to assess and compare their performance. The effect of varying temperature on partially shaded PV modules has also been investigated. The extensive simulation results so obtained have been analyzed. From the results, it has been observed that OEC offers the minimum power loss, highest FF and best performance ratio for all the partial shading cases considered. The major concluding points are as follows:

- The proposed reconfiguration method of OEC is found to be superior in efficiency than all the other configurations, with maximum reduction in mismatch power loss of 518 W for ASY and TCT configurations and 452 W for BL-TCT configuration, maximum increase in fill factor by 19.33% for ASY and TCT configurations and 16.46% for BL-TCT configuration and a maximum performance ratio of 87.9% for the considered partial shading conditions.
- Hence, it has been concluded that the proposed OEC reconfiguration method offers improved performance over other configurations, such as the ASY and TCT configurations, for the considered PSCs of a diagonally progressing shadow movements.

Declaration of competing interest

The authors declare that they have no known competing financial interests or personal relationships that could have appeared to influence the work reported in this paper.

CRediT authorship contribution statement

Karan Yadav: Conceptualization, Software, Visualization, Investigation. **Bhavnesh Kumar:** Supervision, Methodology, Writing - original draft. **Swaroop D.:** Writing - review & editing.

References

Ashouri-Zadeha, Alireza, Toulabia, Mohammadreza, Dobakhsharib, Ahmad Salehi, Taghipour-Broujenia, Siavash, Ranjbara, Ali Mohammad, 2018. A novel technique to extract the maximum power of photovoltaic array in partial shading conditions. Int. J. Electr. Power Energy Syst. 101, 500–512.

Bishop, J.W., 1988. Computer simulation of the effects of electrical mismatches in photovoltaic cell interconnection circuits. Sol. Cells 25 (1), 73–89.

de Blas, M.A., Torres, J.L., Prieto, E., García, A., 2002. Selecting a suitable model for characterizing photovoltaic devices. Renew. Energy 25 (3), 371–380.

Deshkar, Shubhankar Niranjan, Dhale, Sumedh Bhaskar, Mukherjee, Jishnu Shekar, Sudhakar Babu, T., Rajasekar, N., 2015. Solar PV array reconfiguration under partial shading conditions for maximum power extraction using genetic algorithm. Renew. Sustain. Energy Rev. 43, 102–110.

Indu Rani, B., Saravana Ilango, G., Nagamani, Chilakapati, 2013. Enhanced power generation from PV array under partial shading conditions by shade dispersion using Su Do Ku configuration. IEEE Trans. Sustain. Energy 4 (3), 594–601.

Karatepe, Engin, Boztepe, Mutlu, Colak, Metin, 2007. Development of a suitable model for characterizing photovoltaic arrays with shaded solar cells. Sol. Energy 81 (8), 977–992.

Kovach, A., Schmid, J., 1996. Determination of energy output losses due to shading of building-integrated photovoltaic arrays using a raytracing technique. Sol. Energy 57 (2), 117–124.

Malathy, S., Ramaprabha, R., 2015. A static PV array architecture to enhance power generation under partial shaded conditions. Proceedings of IEEE Conference on Power Electronics and Drives System. pp.341–346.

Mishra, Neha, Yadav, Anurag Singh, Pachauri, Rupendra, Chauhan, Yogesh K., Yadav, Vinod K., 2017. Performance enhancement of PV system using proposed array topologies under various shadow patterns. Sol. Energy 157, 641–656.

Potnuru, Srinivasa Rao, Pattabiraman, Dinesh, Ganesan, Saravana Ilango, Chilakapati, Nagamani, 2015. Positioning of PV panels for reduction in line losses and mismatch losses in PV array. Renew. Energy 78, 264–275.

Quaschning, Volker, Hanitscht, Rolf, 1996. Numerical simulation of current–voltage characteristics of photovoltaic systems with shaded solar cells. Sol. Energy 56 (6), 513–520.

Shams El-Dein, M.Z., Kazerani, M., Salama, M.M.A., 2011. Novel configurations for photovoltaic farms to reduce partial shading losses. In: Proceedings of IEEE International Conference on Power and Energy Society General Meeting. pp. 1–5.

Vijayalekshmy, V., Bindu, G.R., Iyer, S.R., 2015. Performance improvement of partially shaded photovoltaic arrays under moving shadow conditions through shade dispersion. J. Inst. Eng. (India) Ser. B 96, 1–7.

Vijayalekshmy, S., Bindu, G.R., Rama Iyer, S., 2016. A novel Zig-Zag scheme for power enhancement of partially shaded solar arrays. Sol. Energy 135, 92–102.

Villa, Luiz Fernando Lavado, Picault, Damien, Raison, Bertrand, Bacha, Seddik, Labonne, Antoine, 2012. Maximizing the power output of partially shaded photovoltaic plants through optimization of the interconnections among its modules. IEEE J. Photovolt. 2 (2), 154–163.

Yadav, Anurag Singh, Pachauri, Rupendra Kumar, Chauhan, Yogesh K., Choudhury, S., Singh, Rajesh, 2017. Performance enhancement of partially shaded PV array using novel shade dispersion effect on magic-square puzzle configuration. Sol. Energy 144, 780–797.